Journal of Alloys and Compounds 697 (2017) 341–352

Contents lists available at ScienceDirect

Journal of Alloys and Compounds

journal homepage: http://www.elsevier.com/locate/jalcom

Effect of solution heat treatment on microstructure and damage accumulation in cast Al-Cu alloys

R. Fernández Gutiérrez [a, *], F. Sket [b], E. Maire [c], F. Wilde [d], E. Boller [e], G. Requena [f]

[a] Nemak Linz GmbH, Zeppelinstraße 24, 4030, Linz, Austria
[b] IMDEA Materials, Eric Kandel 2, Tecnogetafe, 28906, Getafe, Spain
[c] INSA-Lyon, MATEIS CNRS UMR5510, F-69621 Villeurbanne, France
[d] Helmholtz-Zentrum Geesthacht, Center for Materials and Coastal Research, Max-Planck Straße 1, 21502, Geesthacht, Germany
[e] European Synchrotron Radiation Facility, 6 Rue Jules Horowitz, BP 220, F-38043, Grenoble Cédex, France
[f] Department of Metals and Hybrid Materials, Institute of Materials Research, German Aerospace Center, Linder Höhe, 51147, Cologne, Germany

ARTICLE INFO

Article history:
Received 1 June 2016
Received in revised form
27 October 2016
Accepted 19 November 2016
Available online 21 November 2016

Keywords:
Metals and alloys
Synchrotron radiation
Intermetallics
Metallography
Mechanical properties

ABSTRACT

The influence of solution treatment time on the microstructure of three cast Al-Cu alloys is investigated in terms of the effect on damage accumulation during tensile deformation at room temperature. The microstructure of the alloys is formed by an age hardenable α-Al matrix and interdendritic aluminides whose volume fraction and interconnectivity depends on the chemical composition and solution treatment time as revealed by 2D and 3D investigations. The damage accumulation process during tensile deformation is investigated in situ by synchrotron microtomography. Aluminides oriented perpendicularly to the load direction play a decisive role in damage formation and accumulation in the form of microcracks for all studied alloys and conditions. However, highly interconnected aluminides promote rapid crack propagation within these networks, indicating that the concentration of Cu should be kept <5 wt% and a solution heat treatment of 4 h at 530 °C should be applied to increase ductility of these cast alloys.

1. Introduction

Al-Si alloys have been the most widely used Al-alloys for manufacturing combustion engine parts due to their low density, good castability, mechanical performance and corrosion resistance [1]. However, alloys that can withstand higher service temperatures than Al-Si alloys are required to cope with current environmental regulations that impose an increase of efficiency of car engines [2–4]. Cast Al-Cu alloys present better mechanical performance than cast Al-Si alloys at temperatures >250 °C and are, consequently, potential alternatives from a mechanical point of view. Nevertheless, they have scarcely been applied in the automotive industry due to their castability and hot tearing problems [4,5].

The strength of cast Al-Cu alloys is mainly given by their age hardening capabilities [1,6]. The microstructure of as cast Al-Cu alloys is formed by an age hardenable α-Al matrix and several types of aluminides in the intergranular regions [7]. The composition of these aluminides depends on the composition of the alloy and the solidification conditions, i.e. primary stable aluminides can be found together with microsegregated phases. Although their influence on the ductility of the alloys has been reported by several groups [6–11], the role played by topological parameters such as interconnectivity on damage accumulation induced by mechanical deformation during tensile loading remains unclear. This requires three dimensional (3D) characterization of both the microstructure and the process of damage [12–18]. In the present work, synchrotron X-ray computed tomography (SXCT) is combined with in situ tensile tests aiming at studying the relationships between the 3D structure of aluminides in cast Al-Cu alloys and the mechanisms of damage accumulation. The investigations are carried out for three alloys with different chemical compositions which result in different microstructures both in as cast condition and after solution heat treatments (ST).

2. Experimental

2.1. Material

The B206, AlCu7 and AF52 alloys with the chemical compositions shown in Table 1 have been investigated. They were produced

* Corresponding author. Nemak Linz GmbH, Zeppelinstrasse 24, A-4030 Linz, Austria.
E-mail address: ricardo.fernandez.guti@gmail.com (R. Fernández Gutiérrez).

http://dx.doi.org/10.1016/j.jallcom.2016.11.280
0925-8388/

Table 1
Chemical composition of the investigated Al-Cu alloys (wt%).

Alloy	Cu	Mn	Mg	Si	Fe	Ti	Zr	Sr	Al
B206	4.8	0.24	0.33	0.13	0.09	0.006	<0.001	0.0002	Bal.
AlCu7	6.5	0.45	0.013	0.07	0.1	0.11	0.22	<0.0001	Bal.
AF52	4.75	0.41	0.0035	0.06	0.08	0.168	0.0009	0.0002	Bal.

by rotatory gravity die casting (Rotacast® [19]) by Nemak Linz GmbH [20]. All the alloys were studied after solution treatment at 530 °C during 0 h, 4 h, 8 h and 16 h followed by air cooling (cooling rate > 3 K/s). After these solution treatments, all samples were overaged during 100 h at 250 °C to stabilize the age hardenable α-Al matrix.

Table 2
Parameters of SCT experiments carried out at ID19/ESRF to study the evolution of the microstructures as a function of solution treatment time.

Experiment/parameters	B206 + AlCu7 (0 h, 4 h, 8 h ST) AF52 (0 h, 4 h ST)	B206 + AlCu7 16 h AF52 *16 h*
Beamline energy	ID19 (ESRF) Pink beam - peak at 17.6 keV	ID19 (ESRF) Pink beam - peak at 17.6 keV
Projections	1500	1000
Voxel size	$(0.28\ \mu m)^3$	$(0.55\ \mu m)^3$
Min. feature size considered for quantification	$0.59\ \mu m^3 = 0.84 \times 0.84 \times 0.84\ \mu m^3 = 27$ vox	$4.5\ \mu m^3 = 1.65 \times 1.65 \times 1.65\ \mu m^3 = 27$ vox
Detector	FReLoN-CCD	PCO-CMOS
Distance sample-detector	5 mm	5 mm
Acquisition time	~5 min	~30 s
Scanned volume	$\sim 0.19\ mm^3 = 573.4 \times 573.4 \times 573.4\ \mu m^3$	$\sim 1.36\ mm^3 = 1108.8 \times 1108.8 \times 1108.8\ \mu m^3$

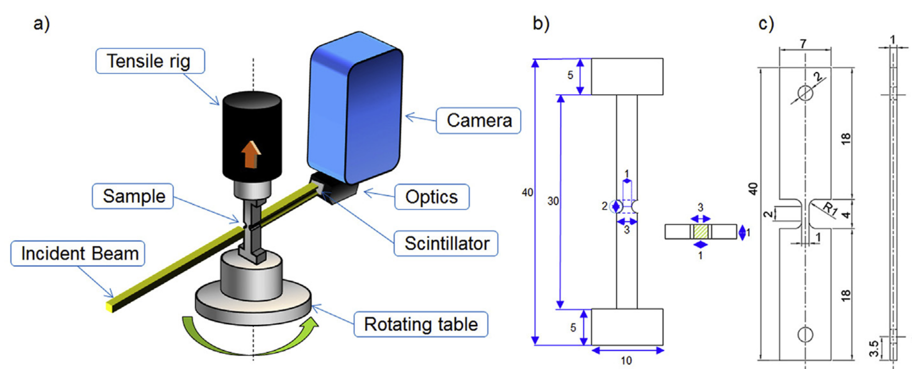

Fig. 1. a) schematic representation of the setup used for the interrupted tensile tests and geometry of the samples used at b) the ID19 and ID15 beamlines of the ESRF and c) P05 of PETRA III.

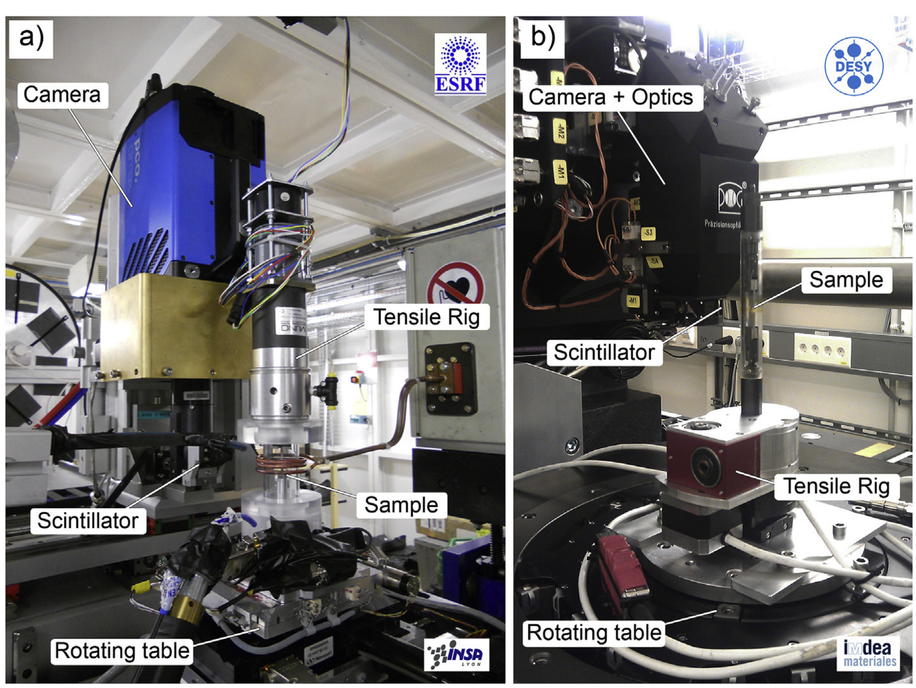

Fig. 2. Experimental setup used for synchrotron tomography experiments during interrupted tensile tests at a) ID15/ESRF and b) at P05/PETRAIII.